

Field studies of wind induced internal pressure in a warehouse with a dominant opening

T.K. Guha^{*}, R.N. Sharma and P.J. Richards

Department of Mechanical Engineering, The University of Auckland, Private Bag 92019, Auckland, New Zealand

(Received September 24, 2011, Revised February 8, 2012, Accepted March 12, 2012)

Abstract. A field study of wind-induced internal pressures in a flexible and porous industrial warehouse with a single dominant opening, of various sizes for a range of moderate wind speeds and directions, is reported in this paper. Comparatively weak resonance of internal pressure for oblique windward opening situations, and hardly discernible at other wind directions, is attributed to the inherent leakage and flexibility in the envelope of the building in addition to the moderate wind speeds encountered during the tests. The measured internal pressures agree well with the theoretical predictions obtained by numerically simulating the analytical model of internal pressure for a porous and flexible building with a dominant opening. Ratios of the RMS and peak internal to opening external pressures obtained in the study are presented in a non-dimensional format along with other published full scale measurements and compared with the non-dimensional design equation proposed in recent literature.

Keywords: internal pressure; warehouse; field study; Helmholtz resonance; leakage; flexibility; porous and flexible building; non-dimensional design equation

1. Introduction

The wind loading on most structural elements of a building are a result of the combination of external and internal pressures. In addition, wind induced internal pressures play an important role in the design of naturally ventilated buildings for indoor air-flow characteristics, humidity, temperature, fire safety and smoke-control issues. Internal pressures are transmitted in buildings through envelope flexibility, leakages and/or dominant openings in response to spatially and temporally varying wind induced external pressures. In the presence of dominant opening(s), internal pressure is known to exhibit a dynamic response to fluctuating external pressure near the opening. The resulting internal pressure in combination with the external pressure can significantly exacerbate the net load on the building envelope or cladding(s). This is especially so in cyclone-prone areas where there is a higher probability of opening creation either by debris impact or by direct wind loading. Different aspects of the behavior of internal pressure of small and large flexible buildings with single and multiple openings and background leakage, such as the Helmholtz resonance, have been theoretically and experimentally investigated by several authors

^{*}Corresponding author, Graduate student, E-mail: tguh001@aucklanduni.ac.nz

(Holmes 1979, Liu and Saathoff 1982, Vickery and Bloxham 1992, Sharma and Richards 1997), and the possibility of occurrence of strong internal pressure resonance has been reported. While the strongest resonance of internal pressure due to turbulent buffeting is expected for an onset flow normal to the opening, Sharma and Richards (2003) have shown using wind tunnel tests that an even stronger resonance of internal pressure driven by "eddy dynamics" is possible at oblique flow angles under certain conditions. Many of these past studies (for e.g., Oh *et al.* 2007, Sharma and Richards 2003) also suggested possible inadequacies of the design provisions of internal pressure in the current wind loading standards such as the AS/NZS 1170.2.2002 (2002) for buildings with openings. These studies, with the exception of a few (e.g., Fahrash and Liu 1990, Kwok and Hitchcock 2009) however, are based on wind tunnel and idealized full-scale tests (Ginger *et al.* 1997) involving buildings of the size of domestic dwellings or small workshops, and thus fail to incorporate the typical range of building and environmental conditions encountered in practice. Their recommendations therefore, might prove to be overly conservative for the design of a vast range of semi-engineered low-rise structures, with comparatively larger internal volume, background leakage and inherent envelope flexibility, such as that for a warehouse.

Hence, for the estimation of safe yet realistic and comprehensive design provisions of internal pressure for low-rise buildings, it is desirable to carry out full scale measurements involving such representative buildings. This paper presents the field measurements of internal pressures in a medium sized industrial building, the Twisted Flow Wind Tunnel (TFWT) building of the University of Auckland (UoA) for a range of dominant opening sizes and wind directions, taken from October, 2009-April, 2010. Data obtained in the study is compared with the numerical predictions of internal pressure response based on the analytical model for a porous and flexible envelope. Finally internal pressure statistics obtained are presented in non-dimensional format for comparison with other full scale studies and design equations recently proposed by Holmes and Ginger (2009).

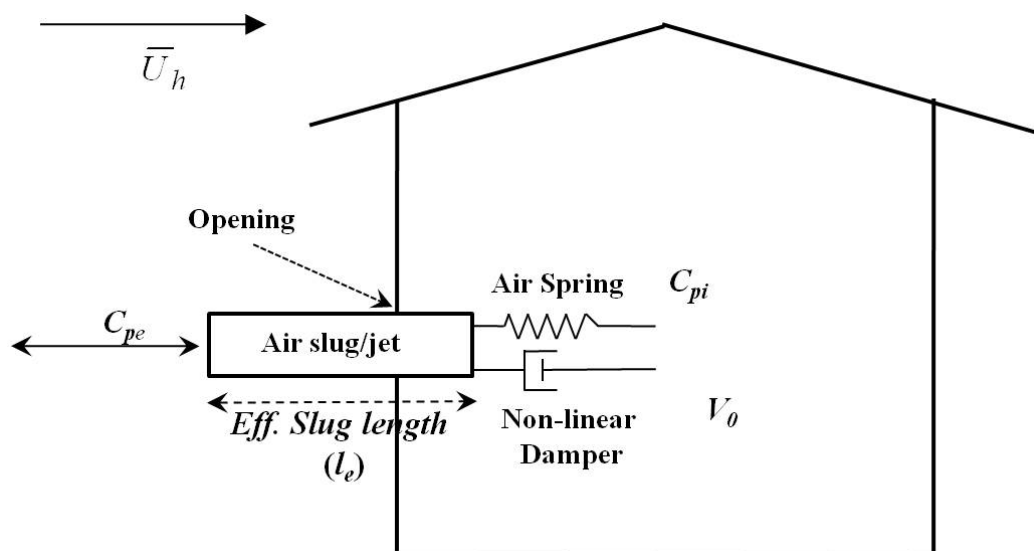


Fig. 1 Air slug model (Holmes 1979)

2. Theoretical considerations

2.1 Governing equations

The first mathematical treatment of the dynamics of internal pressure in buildings with a dominant opening was presented by Holmes (1979). In this seminal paper, a model for the internal pressure resonant response to wind induced turbulent external pressure fluctuations near the opening was proposed. The theory supported by wind tunnel experiments showed that an analogy based on the Helmholtz acoustic resonator can be used to describe the response of internal pressure in a rigid non-porous building using a second order non-linear differential equation. Fig. 1 shows a schematic of the proposed model.

The derivation assumed a “slug” of air to oscillate at the opening under the forcing of external fluctuating pressure, the stiffness being provided by the internal volume of air acting as a pneumatic spring and damped by the irrecoverable energy lost due to flow past the opening. Vickery (1994) further extended the model to include the effect of building flexibility on internal pressure fluctuations. These along with important theoretical contributions from Liu and Saathoff (1982), Vickery and Bloxham (1992), Sharma and Richards (1997), Oh *et al.* (2007) supported by wind tunnel (Sharma and Richards 2003, Oh *et al.* 2007) and some full scale studies (Ginger *et al.* 1997, Fahrash and Liu 1990, Kwok and Hitchcock 2009) by others have greatly led to the development of a sound theoretical basis for internal pressure dynamics. A second order ordinary differential equation with non-linear damping of the form

$$\frac{\rho_a l_e V_e}{\gamma P_a c A_0} \ddot{C}_{pi} + C_L \frac{\rho_a q V_e^2}{2(\gamma P_a A_0)^2} |\dot{C}_{pi}| \dot{C}_{pi} + C_{pi} = C_{pe} \quad (1)$$

has been established by the researchers to model the wind induced internal pressure response of a building cavity with an opening. In this equation, A_0 is the cross-sectional area of the air-slug of effective length $l_e = \sqrt{\pi A_0}/4$, ρ_a is the density of fluid (air in this case) inside the building cavity; V_e is the effective volume of the cavity, being equal to V_0 (the nominal cavity volume) for a building with rigid envelope, and equal to $V_0(1+b)$ for a building with quasi-statically flexible envelope (b being the ratio of the bulk modulus of air inside the cavity to that of the building envelope); $\gamma = 1.4$ is the ratio of specific heat capacities; P_a is the ambient pressure of air; c and C_L are the flow contraction and loss coefficients of flow through the opening; $q = 0.5\rho_a \bar{U}_h^2$ is the ridge height dynamic pressure for a ridge height velocity of \bar{U}_h ; and $C_{pi} = p_i/q$ and $C_{pe} = p_e/q$ are the internal and external pressure coefficients respectively. It is worth noting that significant differences regarding appropriate values for the ill-defined parameters (c , C_L and l_e) still exist to date, with Holmes’ model consisting of a discharge coefficient (k^2) in the denominator of the damping term in Eq. (1) instead of the loss coefficient (C_L).

The undamped resonant frequency (also known as the Helmholtz frequency) is given by

$$f_{hh} = \frac{1}{2\pi} \sqrt{\frac{\gamma P_a c A_0}{\rho_a l_e V_e}} = \frac{1}{2\pi} \sqrt{\frac{\gamma P_a c A_0}{\rho_a l_e V_0 (1+b)}} \quad (2)$$

Eq. (1) implies that under favourable forcing by the external pressure (i.e., with enough turbulence energy) near the opening, the internal pressure can exhibit a significant resonating response at the Helmholtz frequency (given by Eq. (2)) of the cavity-opening combination much like the dynamic response of a structure under the fluctuating wind load.

Guha *et al.* (2011) further extended the model of internal pressure response to include the damping effect of background leakage by incorporating additional terms in Eq. (1). The resulting model

$$\begin{aligned} & \underbrace{\frac{V_0(1+b)\rho_a l_e}{\gamma P_a c A_0} \ddot{C}_{pi}}_{\text{Inertial Term}} + \underbrace{\frac{l_e}{\bar{U}_h c \sqrt{C'_L}} \left(\frac{A_L}{A_0} \right) \frac{\dot{C}_{pi}}{\sqrt{(C_{pi} - \bar{C}_{peL})}}}_{\text{Pseudo-linear Damping Term}} \\ & + \underbrace{\left(\frac{C_L V_0^2 (1+b)^2 \rho_a q}{2(\gamma P_a A_0)^2} \left| \dot{C}_{pi} + \frac{2A_L \gamma P_a}{\rho_a \bar{U}_h V_0 (1+b) \sqrt{C'_L}} [(C_{pi} - \bar{C}_{peL})]^{1/2} \right| \right.}_{\text{Non-linear Damping Term}} \\ & \left. + \left(\dot{C}_{pi} + \frac{2A_L \gamma P_a}{\rho_a \bar{U}_h V_0 (1+b) \sqrt{C'_L}} [(C_{pi} - \bar{C}_{peL})]^{1/2} \right) \right) \\ & = \underbrace{C_{pe}}_{\text{Forcing Function}} - \underbrace{C_{pi}}_{\text{Stiffness Term}} \quad (3) \end{aligned}$$

in which C'_L is the representative loss coefficient through the lumped leakage of area A_L and \bar{C}_{peL} is the area averaged mean external pressure coefficient near the leeward wall respectively, is based on lumping the leakages into a single lumped opening (A_L) on the leeward wall as shown in Fig. 2.

This lumped leakage model results in a damping term [the Pseudo-linear Damping term in Eq. (3)] proportional to the total leakage area in the building envelope. This is in addition to the non-linear damping augmented further by the presence of background porosity in Eq. (3). These additional dampers can severely limit the magnitude of internal pressure fluctuations in real buildings with intrinsically flexible and porous envelope. It should be noted that building porosity has been quantified using porosity ratio (r) defined as A_L/A_0 in the paper.

2.2 Non-dimensional form of the governing equation

A non-dimensional form of the governing equation of internal pressure given by Eq. (1) was proposed by Ginger *et al.* (2008) using the non-dimensional parameters $S^* [= (A_0^{3/2}/V_e)(a_s/\bar{U}_h)^2]$, where a_s is the speed of sound] and $\varphi_5 [= \lambda_U/\sqrt{A_0}]$, λ_U is the longitudinal integral length scale of turbulence at the building ridge height] introduced by Holmes (1979) and a non-dimensional time as

$$t^* [= t\bar{U}_h/\lambda_U]$$

$$\frac{C_I}{cS_*\phi_5^2} \frac{d^2 C_{pi}}{dt_*^2} + \frac{C_L}{4(S_*\phi_5)^2} \left| \frac{dC_{pi}}{dt_*} \right| \frac{dC_{pi}}{dt_*} + C_{pi} = C_{pe} \quad (4)$$

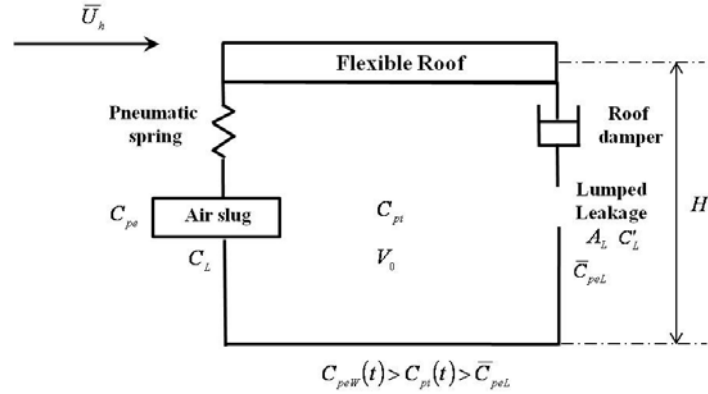


Fig. 2 Air slug model for a leaky and flexible building (Guha *et al.* 2011)

Eq. (4), where C_I is the inertia coefficient of flow through the opening and equal to $\sqrt{\pi/4}$ for steady flow situation, shows that a unique solution of internal pressure variation forced by the external pressure fluctuations (C_{pe}) for a given value of c , C_I , C_L , S^* and ϕ_5 is possible and can be represented by a family of curves of the fluctuating internal pressure (Ginger *et al.* 2008) as a function of variables S^* and ϕ_5 .

A similar exercise with Eq. (3) results in the following non-dimensional expression

$$\frac{C_I}{cS_*\phi_5^2} \frac{d^2 C_{pi}}{dt_*^2} + \frac{C_L}{4(S_*\phi_5)^2} \left| \frac{dC_{pi}}{dt_*} \right| + 2 \left(\frac{A_L}{A_0} \right) S_* \phi_5 \sqrt{\frac{C_{pi} - \bar{C}_{peL}}{C'_L}} \left(\frac{dC_{pi}}{dt_*} + 2 \left(\frac{A_L}{A_0} \right) S_* \phi_5 \sqrt{\frac{C_{pi} - \bar{C}_{peL}}{C'_L}} \right) + \left(\frac{A_L}{A_0} \right) \frac{C_I}{\phi_5 c \sqrt{C'_L (C_{pi} - \bar{C}_{peL})}} \frac{dC_{pi}}{dt_*} + C_{pi} = C_{pe} \quad (5)$$

for the analytical model of internal pressure in a flexible and porous building with a dominant opening.

2.3 Non-dimensional design equations

Holmes and Ginger (2009) non-dimensionalised the expression for the ratio of standard deviations of internal and external pressure fluctuations developed by Vickery and Bloxham (1992). External pressure near the opening approximated as a ‘white noise’ was assumed to induce internal pressure fluctuations with a dominant resonant contribution in comparison to the low frequency ‘background’ noise. The non-dimensional equations were found to over-predict the dynamic

component of internal pressure against measured data beyond S^* of about 10 due to over-estimation of the inertial effects of flow through the opening. Similar treatment with the RWDI (1993) expression for the ratio of standard deviations of internal and external pressure fluctuations resulted in an under-prediction at all but small values of S^* due to neglecting of the inertial flow effects. An intermediate bi-linear design equation empirically obtained by fitting the data from wind tunnel tests involving a range of building volumes and opening sizes was proposed (Holmes and Ginger 2009) as

$$\frac{\tilde{C}_{pi}}{\tilde{C}_{pe}} = 1.1 + \left(\frac{4}{\phi_5} \right) \log_{10}(S^*) \quad \text{for } 0.1 < S^* < 1.0 \quad (6a)$$

$$\frac{\tilde{C}_{pi}}{\tilde{C}_{pe}} = 1.1 \quad \text{for } S^* > 1.0 \quad (6b)$$

and further simplified for usage in wind loading provisions using hard-coded values of relevant parameters. These equations were shown to be useful for estimation of peak ratios of internal to external pressure generated by atmospheric turbulence as

$$\frac{\hat{C}_{pi}}{\hat{C}_{pe}} = \frac{1 + 2gI_u \left(\frac{\tilde{C}_{pi}}{\tilde{C}_{pe}} \right)}{1 + 2gI_u} \quad (7)$$

where g is the peak factor (3.5 to 3.8) and I_u is the intensity of turbulence.

3. Test facilities and experimental setup

The Twisted Flow Wind Tunnel building of the University of Auckland, a typical warehouse consisting of a large hall housing the Twisted Flow Wind Tunnel with adjoining office space is located on the outskirts of the city of Auckland, New Zealand in an industrial area at Tamaki flanked by similar structures to its north and the west. The hall of dimensions 35.1 m by 24.9 m by 7 m has two closely spaced roller doors of size 5 m by 4.2 m in its southern wall that opens into a space interspersed with obstructions such as bushes, fences, etc. The site experiences predominantly south-westerly winds with mean hourly speeds in the range of 4-5 m/s being influenced by the presence of Mount Wellington a kilometre away in the southwest. The winds are mostly oblique (40-60° to the wall normal) to the wall containing the opening(s) during such times. North-easterly winds are also common during the summer months (December-March) such that the opening(s) are located in the leeward wall during such events. Of the two roller doors connecting the hall to the exterior, one which could be opened was used for testing purposes. Fig. 3(a) shows the southern wall of the TFWT building with the roller door used for tests partially open in the picture while Fig. 3(b) shows a detailed plan view of the site.

Six pressure pads connected to differential pressure sensors (range $\sim \pm 650$ Pa, XSCL series, operating range ± 4 inch of water ≈ 1 KPa, Honeywell Inc) through plastic vinyl tubings (Y-105 Scanivalve Corp. USA) of internal diameter 1.8mm were externally installed on the outer wall of the hall surrounding the roller door to capture the wind induced external pressure signals near the

opening. Two pressure pads were installed on the internal wall of the hall, one on each side of the opening 0.5 m away, to acquire the internal pressure response. Fig. 4 shows the location of the external and internal pressure taps used in the tests. The roller door was used to create openings of different sizes, namely 0, 50, 80 and 100% of its maximum size (to be subsequently referred to as configurations A_0 , A_{50} , A_{80} and A_{100} respectively). The signals acquired by the 6 m long vinyl tubes connecting each of these pressure taps to the transducer were corrected for tubing induced distortion by the transfer function approach (Irwin *et al.* 1979) in the frequency domain. The transfer function between the 6 m tubes used in the study and a short 10 mm restricted tube, (brass restrictor with internal diameter 0.4 mm) with near unit gain and near zero phase lag up to 220 Hz connected to a transducer, was established from a separate set of calibration tests involving a white noise generator, amplifier and loud-speaker (model CW2196, Linear X Systems). Although the field pressure data hardly contained any energy beyond 10 Hz, calibration tests were carried out up to a frequency of 300 Hz in order to establish the complete frequency characteristics of the 10 mm reference tubing and the transducer. This was to ensure that the reference system, almost resembling a transducer in-situ, provided undistorted frequency response up to/beyond the frequencies of interest i.e., ≤ 10 Hz. Figs. 5(a) and (b) show the pressure pad and the transducers respectively while Fig. 5(c) shows the frequency response of the 10 mm reference tubing and those used for field measurements as obtained from the calibration tests.



(a)



(b)

Fig.3 (a) The TFWT building and the roller doors used for the tests and (b) test site detail in plan (source: Google map)

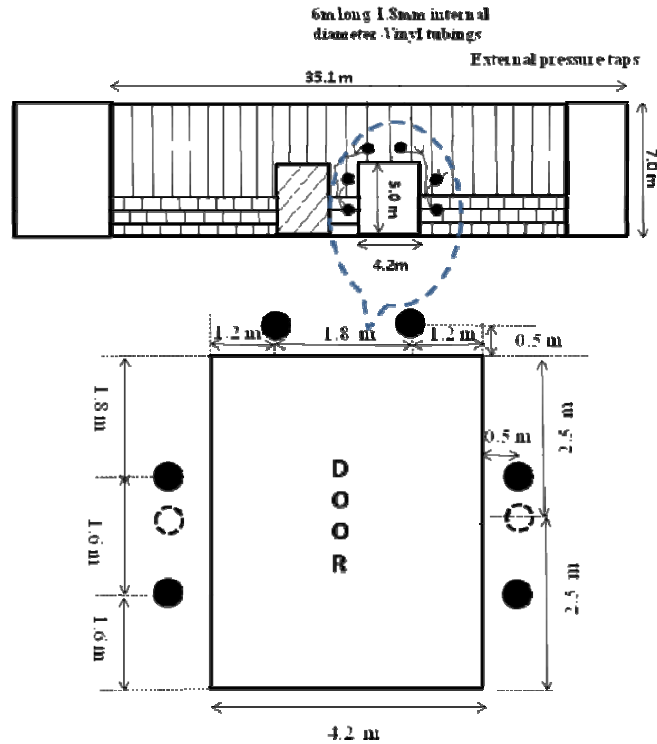


Fig. 4 Location of external pressure taps around the opening on the wall of the TFWT building; External taps in marked in bold (6 nos.) and internal taps marked as dotted (2 nos.)

The differential transducers were referenced to the static pressure measured using a specially designed directional static pressure probe (essentially a pitot tube with a vane attached to its back) installed on a mast at a height of 6 metres and placed south of the opening around 32 m ($=4.5 H$, H being the building height ≈ 7 m) away from the building. The connection, involving ball-bearing joint, of the probe to the mast enabled it to freely rotate about its vertical axis to capture the static pressure by turning into the wind (along the pre-dominant wind direction) at all times. The frequency response of the static (or backing) pressure signals measured by the probe, and transmitted by a rubber tube of length 40m and internal diameter 5 mm to the transducers, was attenuated by incorporating a restrictor/volume damper of time-constant of around 5 seconds (i.e., a frequency response of about 0.2 Hz). Fig. 6 shows a schematic of the probe connected to the mast while facing the predominant wind direction in plan view. Some initial tests involved measurement of reference or static pressure using a wooden box, of dimensions 0.5 m by 0.5 m by 0.5 m, placed on the ground away from the building. This arrangement resulted in significant temperature drift of the pressure signals apparently due to the sensitivity of static pressure to temperature changes. Such effects were however found to be negligible (compared to the uncertainty errors involved in the measurements), with the mean values of 15 minute (pressure) data blocks for a given opening configuration within 10% of each other, when the directional static pressure probe was employed.

An eight channel portable DAQ card (NI USB-6009, National Instruments Inc.) and signal conditioning equipment were used to acquire analog pressure signals digitized and sampled at 32 Hz for storage in the hard disk of a desktop computer equipped with a Pentium 4.2 Ghz processor, 1 GB

ram and 80 GB hard disk. Some acquisition modes also involved sampling at other frequencies, namely 20, 50 and 100 Hz for testing the sensitivity of the instrumentation in picking up the ambient noise in the surroundings. Simultaneous 3 component wind velocity measurements at the building ridge height were carried out using a 3-axis fast response high resolution sonic anemometer (Model Young 81000) placed on the same mast at a height of 7 metres and connected serially (RS-232) to the data logging computer. Prior to tests, the differential pressure transducers were calibrated from the back (i.e., reference) by applying known pressures varying from -150 to +150 Pa.

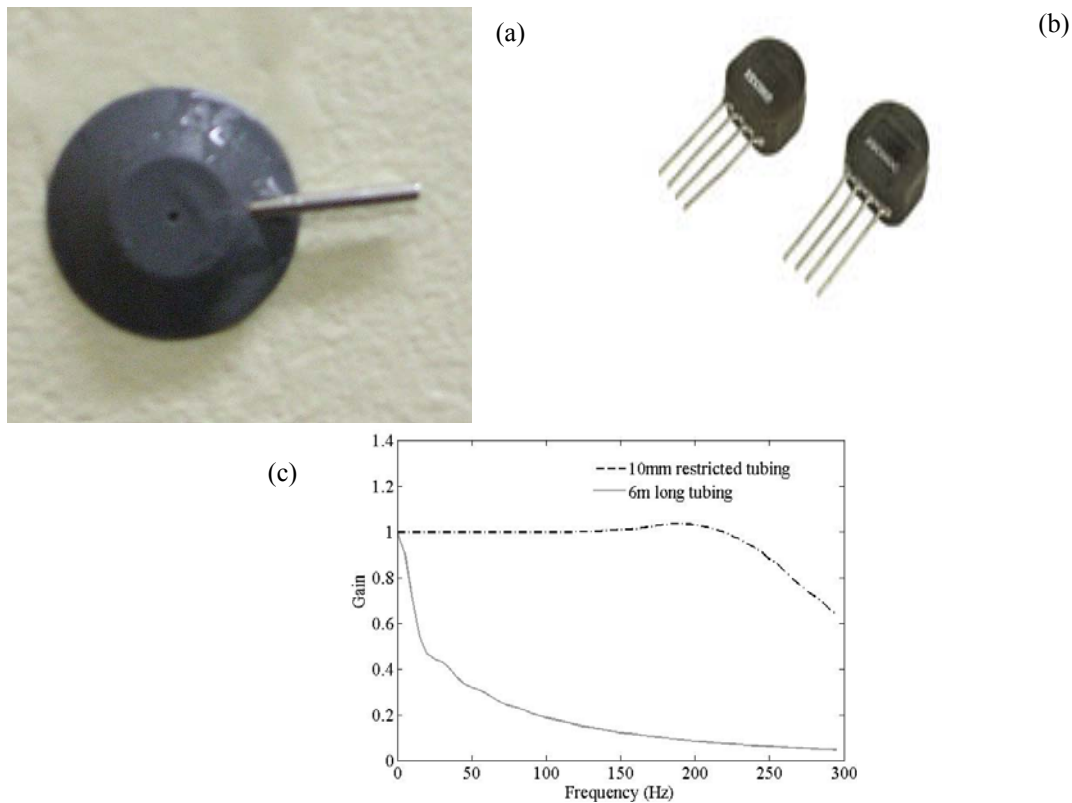


Fig. 5 (a) Plastic pressure pads, (b) Pressure transducers used for field measurements and (c) Frequency response of the reference tubing and that used for field tests for transfer function estimation

A total of 15 relatively moderate windy days from October 2009 to April 2010 were chosen subject to the constraints of resources as well as the availability of wind tunnel hall for testing purposes. The maximum gust wind speeds recorded were in the range of 10-15m/s on the days of the test. Records of wind velocity, external and internal pressure were collected for a period of 1 hour for each of the four different opening sizes tested. Data subjected to further validation procedure involving the calculation of mean statistics of velocity (magnitude and direction) and pressure for a “15minute-block” resulted in the rejection of about 6 days of data that showed non-stationarity as well as temperature drift. It should be noted that prior to the start of each set of test, the transducers were “zeroed” with the building nominally sealed off from the exterior and the offset subtracted from the test data subsequently logged for each opening configuration.

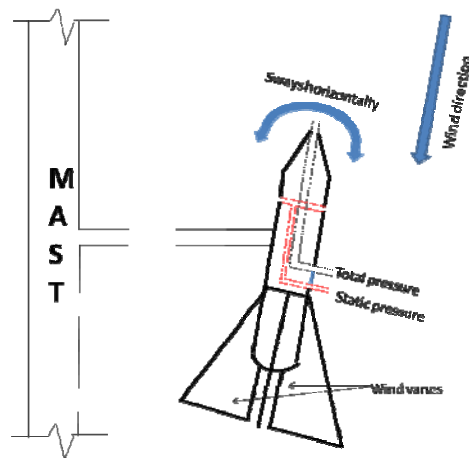


Fig. 6 Schematic of the static pressure probe attached to the mast and facing the wind in plan view

4. Data analysis and results

While data for a wide range of wind directions [see Fig. 3(b) for definition of wind direction θ] including all four quadrants have been obtained in the study (see Table 1), the normally accepted most severe case of wind consistently blowing normally ($\theta=0^\circ$) into the opening has not been obtained. This has partly to do with the nature of wind flow being affected by the local topography of the site as well as due to lack of availability of the test facility during such events.

The mean external pressure coefficients are presented as the ensemble average of all six external pressure taps while the mean internal pressure is calculated as the average of the pressures recorded by two internally installed pressure taps.

Table 1 Statistics of the data acquired during full scale tests

Day of test	Sampling rate (Hz)	Mean hourly speed (m/s)	Mean angle of attack (degrees)	Mean C_{pe} (± 0.05)		Mean C_{pi} (± 0.05)
				$A_{100}/A_{80}/A_{50}/A_0$	$A_{100}/A_{80}/A_{50}$	A_0
22 nd Oct., 09	20	3.10	87	0.002	0.012/-0.019	-0.094/-0.146
23 rd Oct., 09	20	4.35	44	0.367	0.334/0.333	-0.066/-0.082
06 th Nov., 09	20	3.97	40	0.482	0.429/0.430	-0.046/-0.061
09 th Nov., 09	20	4.83	44	0.360	0.345/0.339	-0.090/-0.103
10 th Nov., 09	20	3.15	212	-0.297	-0.263/-0.284	-0.117/-0.138
30 th Nov., 09	100	4.07	113	-0.190	-0.128/-0.144	-0.119/-0.137
03 rd Dec., 09	20,50	4.15	247	-0.306	-0.227/-0.248	-0.158/-0.181
26 th Apr., 10	32	3.39	294	0.293	0.248/0.233	-0.091/-0.120
27 th Apr., 10	32	4.06	227	-0.370	-0.277/-0.299	-0.147/-0.169

200 second pressure traces of the external and internal pressure coefficients obtained on 9th Nov, 2009 for windward configurations A_0 and A_{100} corresponding to wind direction (θ) 44° are shown in Figs. 7(a) and (b) respectively. The measured internal pressure signals are found to follow the trend of external pressure fluctuations near the opening in both cases. While this is expected for A_{100} with the internal taps located on the wall adjacent to the opening, the direct interaction of internal

and external pressures even with the door closed i.e., A_0 , as observed in Fig. 7(a), is due to large crevices and leakage in the interface of the metal-sheeting that lines the upper half of the wall containing the opening. The magnitude of internal pressure fluctuations therefore, is comparatively higher than one might expect for a perfectly sealed building. The mean internal pressure coefficient for configuration A_0 however, is much smaller than the corresponding mean external pressure indicating the role of dominant opening size on the magnitude of mean internal pressure.

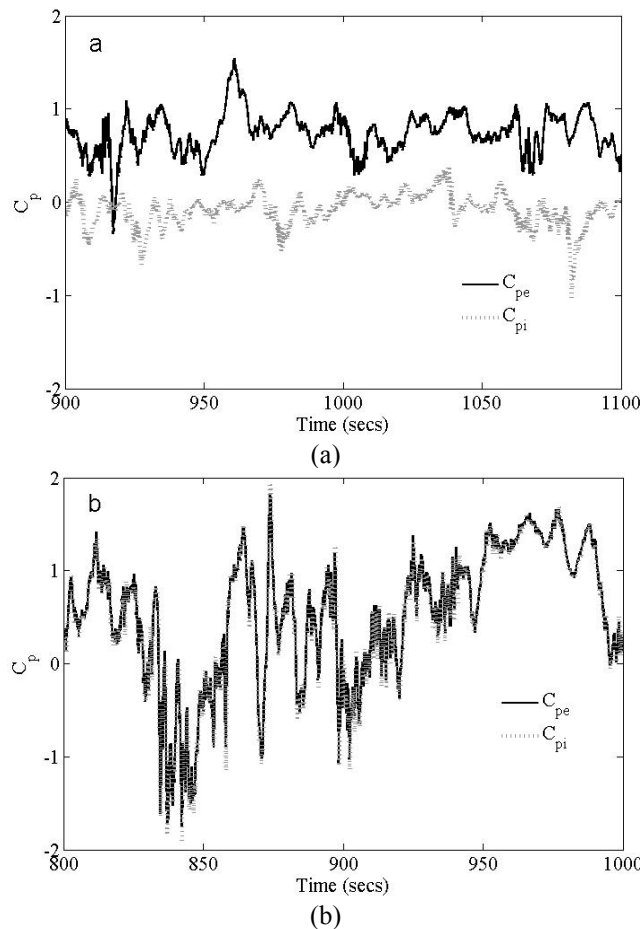


Fig. 7 200 seconds measured external and internal pressure for configurations (a) A_0 and (b) A_{100} for a mean wind angle of 44°

The investigation of the internal pressure dynamics for the building with different opening configurations involved determination of the frequency dependent gain function of internal to external pressure fluctuations for the sampled data. The gain function ($|\chi_{C_{pi}C_{pe}}(f)|$) obtained from the cross-spectral estimates of internal and external pressure signals is calculated as

$$\left| \chi_{C_{pi}C_{pe}}(f) \right| = \frac{\left[C_{C_{pi}C_{pe}}^2(f) + Q_{C_{pi}C_{pe}}^2(f) \right]^{1/2}}{S_{C_{pe}}(f)} \quad (8)$$

where $C_{C_{pi}C_{pe}}(f)$ and $Q_{C_{pi}C_{pe}}(f)$ are the real (Co-spectral) and imaginary (Quadrature) parts of the cross-spectrum of internal and external pressure sampled simultaneously while $S_{C_{pe}}(f)$ is the

auto-spectrum of area averaged external pressure near the opening. Cross-spectral estimates (involving the Quadrature component) were used to eliminate the un-correlated noise in the signals. 50 blocks of 2048 consecutive data samples were used to calculate the gain function in each case.

Figs. 8(a), (b) and (c) each show the plot of frequency dependent gain functions of internal over the area averaged external pressure for configurations A_{100} , A_{80} and A_{30} for the wind directions (θ) 44° , 294° and 247° respectively.

For the first two wind directions, the openings can be seen to be lying on the windward wall; although at oblique wind angles and on opposite sides of the normal. A gain in excess of unity is observed at the Helmholtz frequency of the building volume-opening area combination in these cases with the gains slightly higher for configurations A_{100} and A_{80} in comparison to A_{50} as expected. A very slight increase in the resonant frequency with increase in the windward opening area as predicted by theory is also observed in Figs. 8(a) and (b). However, the magnitude of internal pressure fluctuations at resonance are much less than some of the earlier reported studies and in fact are hardly discernable in the spectra of internal pressure coefficients plotted in logarithmic scale for configuration A_{50} in Fig. 8(d) and to some extent in Fig. 8(e). This may be due to the damping influence of leakage and envelope flexibility inherent in a real industrial building or increased turbulence in the approach wind.

For the case of leeward opening corresponding to wind direction 247° , the gain and spectra of internal pressure coefficient in Figs. 8(c) and (f) does not reveal any discernible Helmholtz resonance for all the opening areas investigated. This is possibly due to comparatively weaker external pressures in the building wake without enough energy to force an internal pressure resonance inside the building with such a large internal volume. Also, unlike the windward opening situations, high frequency fluctuations beyond the theoretical Helmholtz frequency (≈ 1.2 Hz) observed in the gain function plot of Fig. 8(c) is possibly due to high frequency building generated turbulence in the wake.

The spectra of internal pressure coefficient for A_0 , corresponding to the closed dominant opening situation, is found to be much weaker than the others for all wind directions due to absence of the external pressure forcing the internal pressure through the opening. The high frequency noise evident in the internal and external pressure coefficient spectra are probably due to the small range of pressure being measured at moderate wind speeds in comparison to the full range of the sensors but was not filtered out for the fear of removal of useful information. The presence of this high frequency noise effectively disallows the spectra of internal pressure coefficient to fall off sharply beyond the Helmholtz frequency as theoretically predicted.

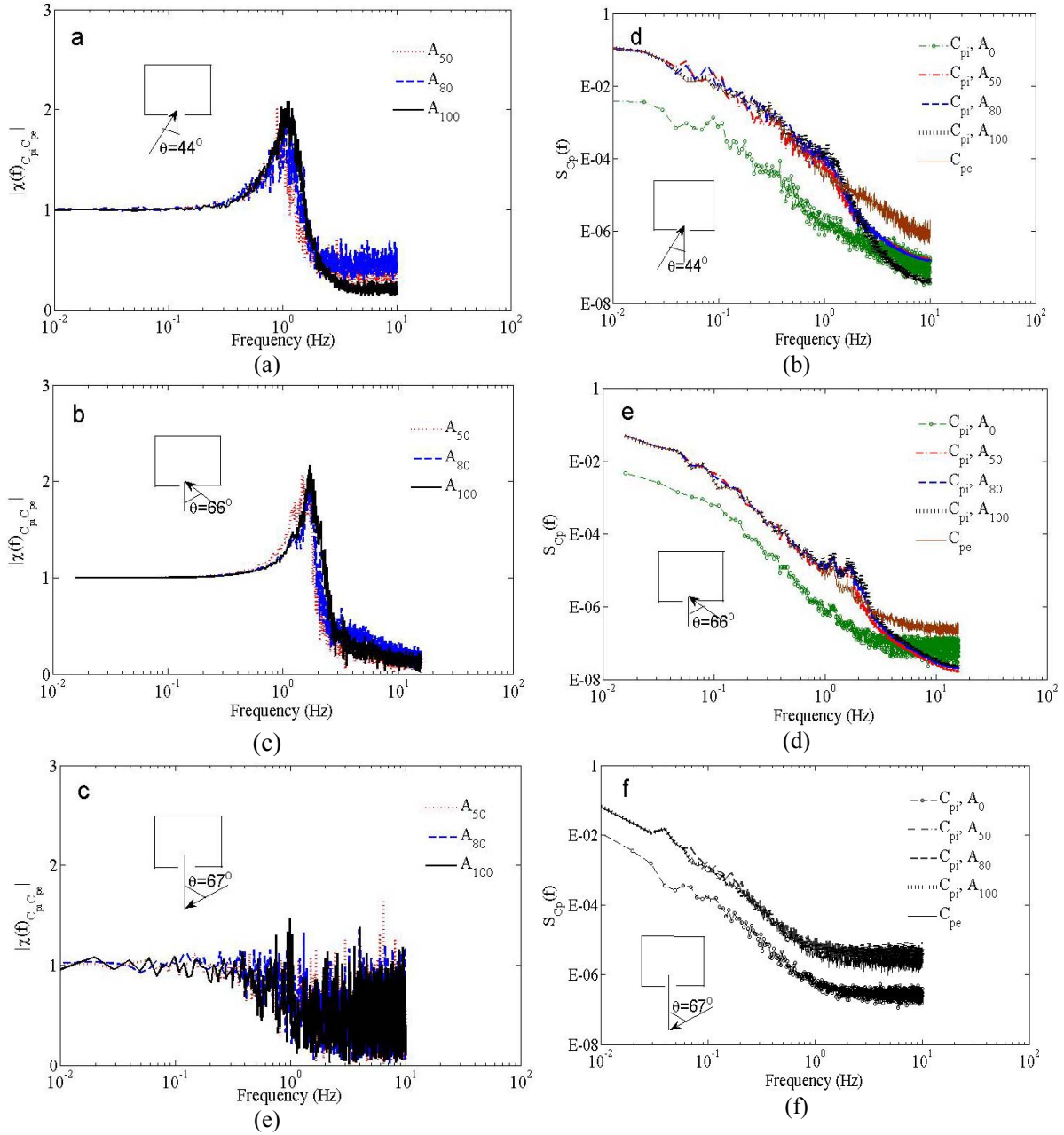


Fig. 8 (a) Gain function of internal over the area averaged external pressure for mean wind directions (a) 44° (b) 294° (66°) and (c) 247° (67°), Spectra of internal and external pressures for wind directions (d) 44° (e) 294° (66°) and (f) 247° (67°) for different opening areas

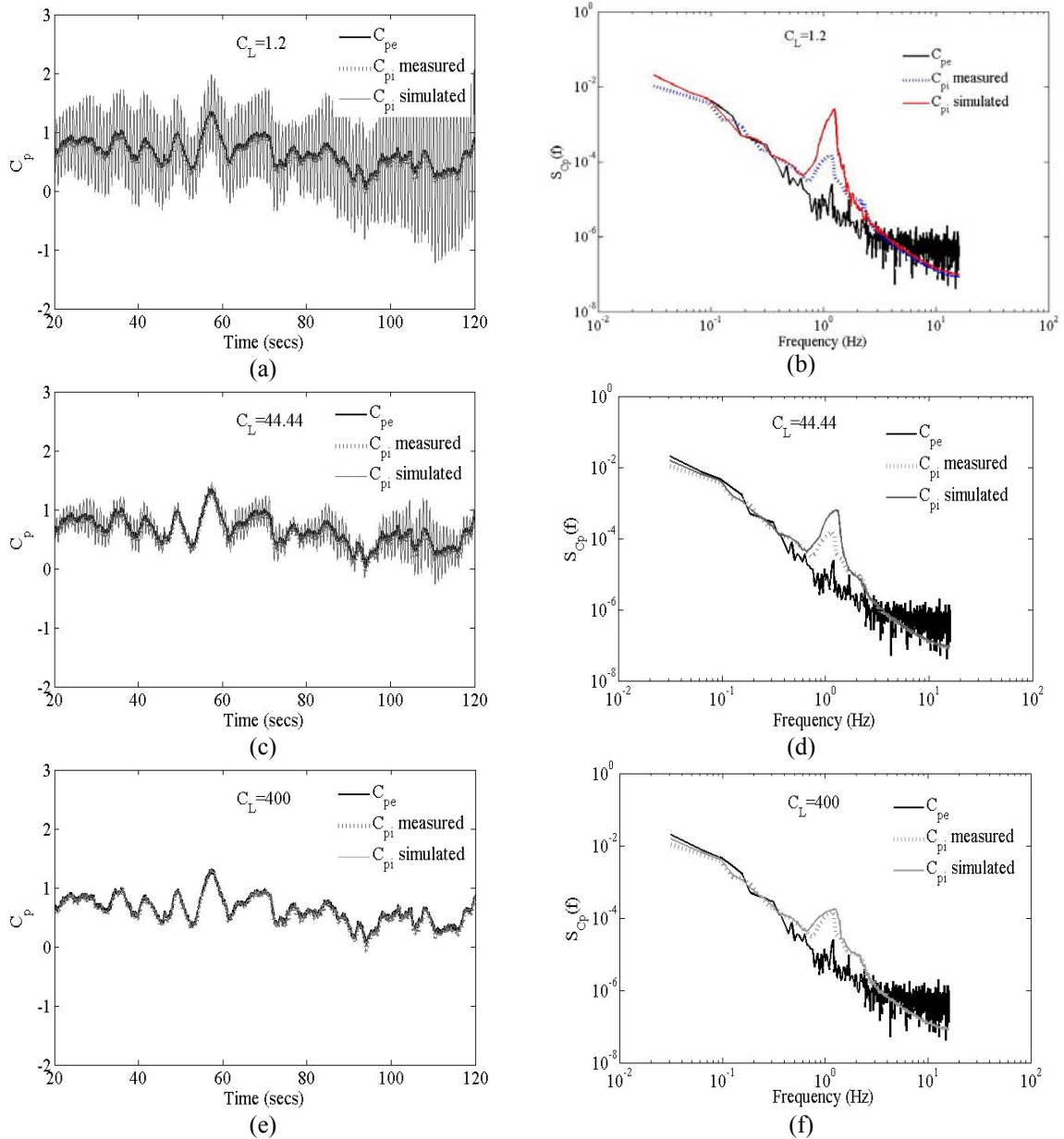


Fig. 9 100 seconds time histories of measured external, internal and simulated internal pressure coefficients using (a) $C_L=1.2$, (b) $C_L=44.44$ and (c) $C_L=400$ and the corresponding spectral densities of measured external, internal and simulated internal pressure coefficients using (a) $C_L=1.2$, (b) $C_L=44.44$ and (c) $C_L=400$ for wind direction 44°

5. Comparison with theory

In order to compare the measured internal pressure response with theoretical predictions, numerical simulations were carried out using Eqs. (1) and (3) for the TFWT building hall. Measured external pressure time histories were used to force the theoretical response of internal pressure. The equations were discretized using a first order explicit backward finite difference scheme [Oh *et al.* (2007)] in which the time derivatives of internal pressures were calculated at each time step j based on C_{pi} values at the preceding two time steps, as shown in Eq. (9), where Δt is the time step.

$$\dot{C}_{pi}^{(j)} = \frac{C_{pi}^{(j)} - C_{pi}^{(j-1)}}{\Delta t}; \ddot{C}_{pi}^{(j)} = \frac{C_{pi}^{(j)} - 2C_{pi}^{(j-1)} + C_{pi}^{(j-2)}}{\Delta t^2} \quad (9)$$

Typically very small time steps of 0.0006 seconds were used for advancing in time in order to minimize the numerical errors. The TFWT hall houses a large open circuit wind tunnel, an acoustic chamber, a large compressor and other equipments that occupy approximately 20% of the free space. Since fan pressurization tests, typically carried out to determine the building porosity and flexibility by internal pressurization using fans, was beyond the resources at disposal due to the large hall size, the value of b that quantifies the envelope flexibility was estimated indirectly from the measured Helmholtz frequency and the approximate nominal internal volume (V_0) of the hall.

Thus, for a nominal hall volume of 4830 m³, measured Helmholtz frequency of 1.2 Hz for A_{100} configuration and standard values of other parameters in Eq. (2), the value of b is estimated to be approximately 0.25. This is within the range of values from 0.2-5 for typical low-rise structures as reported by Vickery (1994). The simulations were carried out under the following basic conditions:

$$V_0 = 4830\text{m}^3, A_0 = 21 \text{ m}^2, l_e = \sqrt{\pi A_0 / 4}, \\ c = 0.6, \rho_a = 1.185\text{kg/m}^3, \gamma = 1.4, P_a = 101300\text{Pa}$$

First set of comparisons involved usage of Eq. (1) by neglecting the presence of leakage in the envelope and attempting to match the theoretical response of internal pressure with the measured data for a windward opening situation ($\theta=44^\circ$) by altering the value of loss coefficient (C_L) through the opening. Figs. 9(a), (b) and (c) show a 100 second record of the measured internal and external pressure coefficient time history along with the simulated internal pressure response for A_{100} configuration using loss coefficient values of 1.2, 44.44 and 400 respectively. Figs. 9(d), (e) and (f) show the corresponding spectral responses of external (measured) and internal (measured and simulated) pressure coefficients. The external pressure taps seem to be partially affected by the resonating internal pressure for this wind direction as evident from the sharp narrow peak in the spectrum of external pressure near the measured Helmholtz frequency of the building. While the value of $C_L=1.2$ has been obtained by Sharma and Richards (1997) and Chaplin *et al.* (2000) using Computational Fluid Dynamics (CFD) and model-scale experiments, Ginger *et al.* (1997) needed a value of $C_L=44.44$ ($k=0.15$ according to Holmes's model) to effect a spectral match between the measured and simulated response of internal pressure for the TTU test setup (Ginger *et al.* 1997) from field measurements. As shown here, both these values of loss coefficient results in over-prediction of the internal pressure response in comparison to the measured data for the TFWT

building.

A much better match is obtained using a loss coefficient value of 400, corresponding to a discharge coefficient k of 0.05. Such a value is however, unrealistic in the opinion of the authors for flow through such a large door, and not supported by previously published data in the literature. Sensitivity analysis carried out by Ginger *et al.* (2010) based on wind tunnel experiments showed a maximum loss coefficient value of 100 ($k=0.1$) for cavity volume-opening area combinations with non-dimensional area to volume ratio (S^*) greater than 10, which still is a higher value when compared to the theoretical estimate of $1/0.6^2=2.78$ (Vickery and Bloxham 1992) obtained from steady potential flow assumptions.

A high loss coefficient value such as the one needed to obtain a reasonable match between theory and experiments in the current study is possibly due to the presence of background leakage, and small vents in the building envelope that acts as additional dampers to the internal pressure. Ideally the loss coefficient should account for only the losses through the dominant opening. However, neglecting the presence of background porosity in simulations using Eq. (1), may have resulted in the loss coefficient being intrinsically influenced by the damping effect of leakage; hence an uncharacteristically high value was obtained.

The envelope of the Twisted Flow Wind Tunnel (TFWT) hall has a number of visible leakage paths, in addition to the usual leakage paths through the corners of doors and those arising out of normal construction tolerances. As mentioned earlier, an indirect estimate of the building leakage had to be undertaken due to inability to carry out fan pressurization tests for such a large hall. In particular, the hall has two large crevices of average width approximately 2 cm that run parallel to the longer wall containing the dominant opening and along the shorter eastern wall. In both of these, one crevice is located at the interface between the lower-half of the wall made of brick and the upper corrugated metal-sheeting. The second is located near the edge of the wall and the roof. These crevices, as mentioned earlier, are responsible for establishing flow paths between the building interior and exterior even for a nominally sealed situation. As a result, contrary to expectations, the internal pressure trace for A_0 (closed dominant opening situation) configuration follows somewhat the trend of the fluctuating external, albeit with a reduced fluctuating response as evident from the internal pressure coefficient spectra in Fig. 8. A porosity ratio (r) of around 8~9% resulting from these crevices for A_{100} configuration was further increased to 10% to account for other leakage paths in numerical investigations.

A second set of simulations were carried out using Eq. (3) to additionally account for the damping influence resulting from these leakages. A value of $C'_L=2.78$ for the lumped leakage and a mean leeward external pressure coefficient (\bar{C}_{peL}) of -0.15 was used for simulations in addition to the parameters already used in the first comparison. Value of the mean leeward external pressure coefficient (\bar{C}_{peL}) corresponding to mean wind direction $\theta=44^\circ$ was obtained from wind tunnel experiments involving a 1:100 scale rigid, non-porous model of the same building under Category 3 (AS/NZS 1170.2.2002) terrain conditions. Fig. 10(a) presents a 100 second trace of the simulated internal pressure coefficient response along with the measured internal and external pressure coefficient using a loss coefficient of 1.2. Fig. 10(b) presents the corresponding auto-spectrum of the measured and simulated internal pressure coefficients. The match between theory and experiments is found to be satisfactory and as good as the simulations carried out using $C_L=400$ in absence of background leakage.

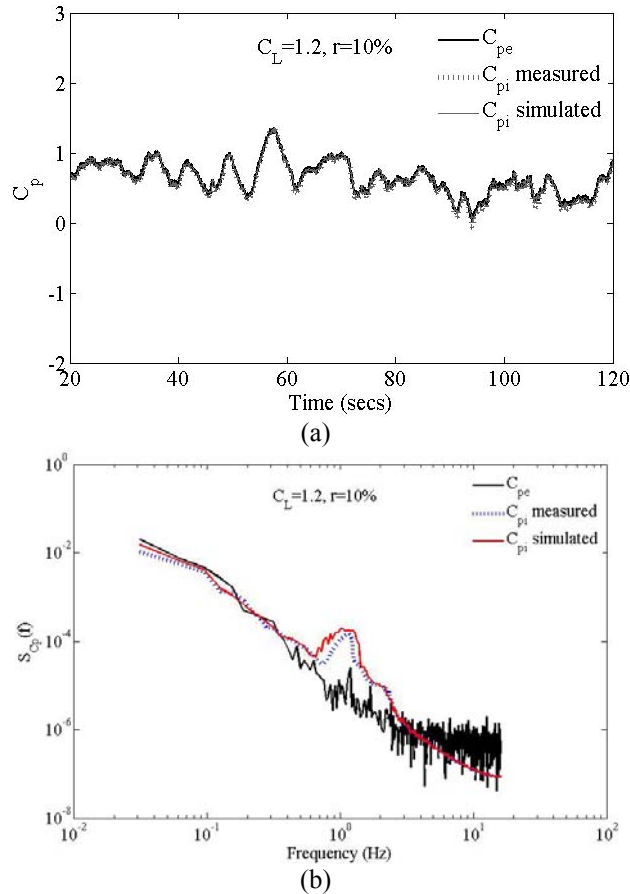


Fig. 10 (a) 100 seconds time histories and (b) Auto-spectrum of measured external, internal and simulated internal pressure coefficients using $C_L=1.2$ and $r=10\%$ for wind direction 44°

This is a more realistic representation of the TFWT building with inherently porous and flexible envelope, and the internal pressure response is simulated using a loss coefficient value that is supported by previous experimental data. This analysis also confirms our previous assumption of C_L being implicitly influenced with the damping effects of leakage, not accounted for in the first set of simulations. A loss coefficient of 44.4 used to match the predictions with the measured internal pressure response by Ginger *et al.* (1997) for the TTU building might possibly incorporate the damping effect of background leakage to some extent as well. An area ratio (i.e., sum of the leakage to the wall area) of 2.5×10^{-4} for the TTU building approximately results in a porosity ratio (r) of 2.3% for the door opening ($A_o=1.94 \text{ m}^2$). Accounting for damping due to this background porosity will probably result in a smaller, more plausible value of C_L .

In other words, for turbulent reversing type flow situations as occurs in the case of internal pressure in buildings through dominant openings, while the values of C_L will be different to that of its steady-state value, influence of other dampers such as envelope flexibility and background leakage should be given due consideration during analysis.

6. Comparison with non-dimensional design equation

Field data of fluctuating internal pressure obtained in the current study along with those reported by other researches (Fahrtash and Liu 1990, Ginger *et al.* 1997) are presented in non-dimensional format for a quantitative comparison. The longitudinal integral length scale of velocity obtained from the sonic anemometer measurements at the ridge height of the building was found to vary from 18 m to 30 m in the current study. An average value of $\lambda_U=25$ m was thus used for estimation of φ_5 with values of 5.5, 6.1, 7.7 and Infinity (nominally sealed) for A_{100} , A_{80} , A_{50} and A_0 configurations respectively. In particular, the ratio of the root-mean-square (RMS) internal to opening external pressures are plotted against the non-dimensional opening area to volume ratio (S^*) in Fig. 11(a) along with the empirical design equation (Eq. (6)) proposed by Holmes and Ginger (2009) for φ_5 of 5 and 160 corresponding to the extremes of the opening sizes used in all full scale studies-past and present.

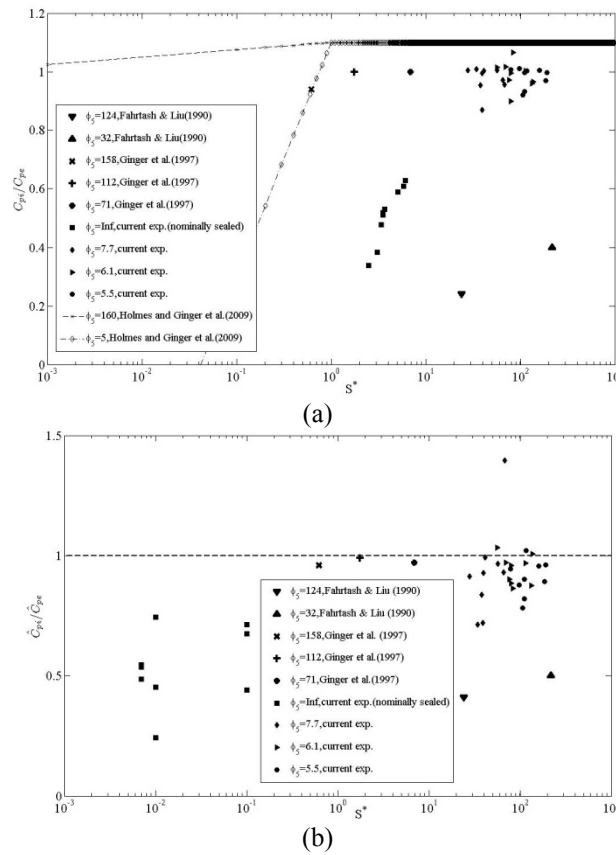


Fig. 11 (a) RMS and (b) Peak ratio of internal to external pressure from full scale measurements

While the prediction model of Holmes and Ginger (2009), based on wind tunnel studies, appear reasonably conservative in comparison to full scale data for values of S^* greater than 1, it must be noted that the full-scale measurements in all three cases in the current study were obtained for oblique wind directions. In addition, the highly fluctuating nature of the wind speed and direction experienced during full scale measurements results in somewhat non-stationary effects. In contrast,

results of the wind tunnel studies using volume scaled rigid non-porous models immersed in unidirectional and stationary boundary layer flow, though conservative, can provide more reliable and safe estimates of dynamic internal pressures under high wind design conditions. The generally smaller RMS internal to external pressure ratios for all values of S^* and ϕ_5 measured in the field in comparison to the prediction model (Eq. (6)) also highlight the damping effects of envelope flexibility and background leakage on internal pressure fluctuations in real leaky and flexible buildings.

It is also worth noting that the prediction model of Holmes and Ginger (2009) is valid for buildings with S^* and ϕ_5 greater than 0.1 and 10 respectively. Though not usually encountered in practice, values of S^* lower than 0.1 are possible for very large industrial buildings such as hangars etc. in cyclonic regions with particularly high design wind speeds. The peak ratios of internal to external pressures measured in full scale are presented in a similar non-dimensional format against S^* in Fig. 11(b) and shows relatively greater scatter, possibly due to the fluctuating nature of wind speeds and directions encountered during field measurements.

7. Conclusions

Full scale investigations of wind induced internal pressure in a warehouse, the Twisted Flow Wind Tunnel building of the University of Auckland, involving a range of dominant opening sizes and wind directions have been carried out at moderate wind speeds. Helmholtz resonance of internal pressure was found to be less pronounced than previously reported studies when there is an oblique windward opening and is hardly discernable at other times; this is attributed to the inherent leakage and flexibility in the envelope of the building, in addition to the moderate wind speeds encountered during the tests. Internal pressure for the nominally sealed situation was found to follow somewhat, the trend of external pressure traces in the study, but with reduced fluctuations; this is again due to large porosity in the building envelope.

Numerical investigations carried out using the rigid, non-porous model of internal pressure to match the measured responses in time and spectral domain resulted in an uncharacteristically high loss coefficient value of 400. The measured internal pressures were however, found to agree well with the simulations for a loss coefficient value of 1.2 carried out using the model for flexible and porous envelope, typical of real industrial buildings. An approximate porosity ratio of 10%, used to quantify the effect of background leakage, and a ratio of the bulk modulus of air to that of the building cavity of 0.25, used to quantify the effect of envelope flexibility, was adopted for numerical investigations to match the measured data. The analysis shows the importance of appropriately modeling the different dampers of internal pressure fluctuations such as envelope flexibility and background leakage, in the absence of which, the apparent loss coefficient of the opening will invariably be influenced by other damping mechanisms. This could result in severe over or under-prediction of the internal pressure resonant response, not desirable from a design viewpoint.

Ratios of the RMS internal to opening external pressure obtained in the study are presented in a non-dimensional format along with other full scale measurements for comparison with the non-dimensional design equation proposed in recent literature. The design equation is found to provide reasonably conservative estimates of RMS internal to external pressure ratios across all values of S^* encountered in field measurements. The peak ratios of internal to external pressure plotted against S^* and ϕ_5 are found to exhibit relatively greater scatter in comparison to the RMS

ratios. This is probably due to the highly fluctuating nature of wind speeds and directions encountered during field measurements.

References

- Chaplin, G.C., Randall, J.R. and Baker, C.J. (2000), "The turbulent ventilation of a single opening enclosure", *J. Wind Eng. Ind. Aerod.*, **85**(2), 145-161.
- Fahrtash, M. and Liu, H. (1990), "Internal pressure of low-rise building - field measurements", *J. Wind Eng. Ind. Aerod.*, **36**(2), 1191-1200.
- Ginger, J.D., Mehta, K.C. and Yeatts, B.B. (1997), "Internal pressures in a low-rise full-scale building", *J. Wind Eng. Ind. Aerod.*, **72**, 163-174.
- Ginger, J.D., Holmes, J.D. and Kopp, G.A. (2008), "Effect of building volume and opening size on fluctuating internal pressure", *Wind Struct.*, **11**(5), 361-376.
- Ginger, J.D., Holmes, J.D. and Kim, P.Y. (2010), "Variation of internal pressure with varying sizes of dominant openings and volumes", *J. Struct. Eng.- ASCE*, **136**(10), 1319-1326.
- Guha, T. K., Sharma, R.N. and Richards, P.J. (2011), "On the internal pressure dynamics of a leaky and flexible building with a dominant opening", *Proceedings of the 13th International Conference on Wind Engineering*, Amsterdam, Holland.
- Irwin, H.P.A.H., Cooper, K.R. and Girard, R. (1979), "Correction of distortion effects caused by tubing systems in measurements of fluctuating pressures", *J. Wind Eng. Ind. Aerod.*, **5**(1-2), 93-107.
- Holmes, J.D. (1979), "Mean and fluctuating internal pressure induced by wind", *Proceedings of the 5th International Conference on Wind Engineering*, Colorado State University, USA.
- Holmes, J.D. and Ginger, J.D. (2009), "Codification of internal pressures for building design", *Proceedings of the 7th Asia-Pacific Conference on Wind Engineering*, Taipei, Taiwan.
- Kwok, K.C.S. and Hitchcock, P.A. (2009), "Characterisation of and wind induced-induced pressures in a compartmentalised building during a typhoon", *J. Wind Eng. Ind. Aerod.*, **6**, 30-41.
- Liu, H. and Saathoff, P.J. (1982), "Internal pressure and building safety", *J. Struct. Div.*, **108**(10), 2223-2234.
- Oh, H.J., Kopp, G.A. and Inculet, D.R. (2007), "The UWO contribution to the NIST aerodynamic database for wind loads on low buildings: Part 3. Internal pressures", *J. Wind Eng. Ind. Aerod.*, **95**(8), 755-779.
- Rowan, W. and Davies, I. (1993), *Review of internal pressures on low-rise buildings, Report to Canadian Sheet Steel Institute*, RWDI Report 93-270.
- Standards Australia/Standards New Zealand (2002), *Australian/New Zealand Standard Structural design actions, Part2: Wind Actions - AS/NZS 1170.2:2002*, Standards Australia International Ltd., Sydney, AS and Standards New Zealand, Wellington, NZ.
- Sharma, R.N. and Richards, P.J. (1997), "Computational modelling of the transient response of building internal pressure to a sudden opening", *J. Wind Eng. Ind. Aerod.*, **72**, 149-161.
- Sharma, R.N. and Richards, P.J. (2003), "The influence of Helmholtz resonance on internal pressures in a low-rise building", *J. Wind Eng. Ind. Aerod.*, **91**(6), 807-828.
- Vickery, B.J. and Bloxham, C. (1992), "Internal pressure dynamics with a dominant opening", *J. Wind Eng. Ind. Aerod.*, **41**(1-3), 193-204.
- Vickery, B.J. (1994), "Internal pressures and interactions with the building envelope", *J. Wind Eng. Ind. Aerod.*, **53**(1-2), 125-144.